IEEE Access
Multidisciplinary | Rapid Review | Open Access Journal

Received July 24, 2020, accepted September 19, 2020, date of publication September 22, 2020, date of current version October 6, 2020.

Digital Object Identifier 10.1109/ACCESS.2020.3025919

Input Power Factor Compensation Strategy for Zero CMV-SVM Method in Matrix Converters

HUU-NHAN NGUYEN[1,2], (Member, IEEE), MINH-KHAI NGUYEN[3,4], (Senior Member, IEEE), VAN-QUANG-BINH NGO[5], TAN-TAI TRAN[1], JOON-HO CHOI[1], (Member, IEEE), AND YOUNG-CHEOL LIM[1], (Member, IEEE)

[1]Department of Electrical Engineering, Chonnam National University, Gwangju 61186, South Korea
[2]Institute of Research and Development, Duy Tan University, Da Nang 550000, Vietnam
[3]Department of Electrical and Computer Engineering, Wayne State University, Detroit, MI 48202, USA
[4]Faculty of Electrical and Electronics Engineering, Ho Chi Minh City University of Technology and Education, Ho Chi Minh City 700000, Vietnam
[5]Faculty of Physics, University of Education, Hue University, Thua Thien Hue 530000, Vietnam

Corresponding authors: Joon-Ho Choi (joono@chonnam.ac.kr) and Young-Cheol Lim (yclim@chonnam.ac.kr)

This work was supported in part by the Korea Electric Power Corporation under Grant R18XA04, in part by the Korea Institute of Energy Technology Evaluation and Planning (KETEP), and in part by the Ministry of Trade, Industry and Energy (MOTIE) of South Korea under Grant 20193810100001B.

ABSTRACT The space vector modulation (SVM) method using only rotating vectors is very effective to suppress the common-mode voltage (CMV) for matrix converters (MCs). However, the effect of the input filter on the input power factor (IPF) has not been fully investigated when using this method. This study investigated the effect of the input filter on the displacement angle and proposes an IPF compensation strategy for the zero CMV-SVM method in MCs. The proposed strategy analyzes the duty cycles of rotating vectors under the IPF-compensation condition. Through this analysis, the proposed strategy adjusts the zero vector by using a set of three counterclockwise-rotating vectors or three clockwise-rotating vectors to make all the duty cycles non-negative, ensuring that the zero CMV-SVM method can be applied to compensate the IPF for the MCs. This study also determines the condition to achieve unity IPF for the main power source and the maximum allowable IPF if the above condition is not met. Finally, experimental results are provided to validate the theoretical study.

INDEX TERMS Matrix converter, space vector modulation, zero common-mode voltage, rotating vector, input power factor.

I. INTRODUCTION

In recent years, matrix converters (MCs) with bidirectional power flow capabilities have received considerable attention. In comparison to traditional back-to-back converters, MCs offer more compact and reliable operation owing to the absence of bulky electrolytic capacitors [1], as shown in Figure 1. Therefore, MCs have garnered significant research interest in industry, particularly the aircraft, electric-vehicle, and wind-generation industries [2]–[4]. However, MCs have not been widely applied in practice owing to several issues affecting input-filter design, bidirectional-switch technology, commutation techniques, and the common-mode voltage (CMV) [5]. Among these problems, the CMV between the motor neutral point and power supply ground is the main source of motor winding failure and bearing damage [6]–[8]. Furthermore, it also causes noise and electromagnetic interference problems, affecting surrounding electronic equipment [9].

Several modulation methods have been presented to effectively reduce the CMV for MCs. Among them, space vector modulation (SVM) is currently the most widely used technique owing to its advantageous features such as harmonic performance, flexibility to optimize the switching pattern, and achieving the highest modulation ratio [5], [10]. Two types of SVM methods are based on replacing the MC zero vectors with active vectors [11] or rotating the vectors [12] to reduce the CMV peak value to 42%. In [13], two lower-input line-to-line voltages are used to synthesize the desired output-voltage vector to mitigate the CMV peak value with a lower total harmonic distortion of the output voltage and a reduction in switching loss. However, the proposed method has the disadvantage of a low voltage-transfer ratio (VTR) of less than 0.5. Guan *et al*. presented a modulation SVM method to

The associate editor coordinating the review of this manuscript and approving it for publication was Snehal Gawande.

reduce not only the peak value but also the RMS of the CM by using all valid switching states, including rotating-vector states [14]. Nguyen and Lee proposed an effective modulation scheme, including an SVM method using only rotating vectors and a modified four-step commutation technique, to achieve zero CMV for MCs [15]. More recently, Lei *et al.* suggested a simpler SVM method to accomplish zero CMV by adopting only three clockwise rotating vectors or counterclockwise rotating vectors [16]. However, the performance of the MC when using this method is reduced significantly because the rotating vectors used are very far from the reference output-voltage vector. Among the aforementioned techniques, the modulation scheme in [15] is the most effective solution for eliminating CMV in MCs, from the perspective of the output voltage quality.

Although zero CMV-SVM methods have been realized, there are still some issues to be resolved. Compensating the input power factor (IPF), affected by the input filter, is one of the most important issues to be handled. In practice, an LC filter is connected at the input of the MC to eliminate high-frequency harmonics of the input current and smooth it to satisfy EMI requirements [17]. However, the input filter produces a displacement angle between the source phase voltage and current [18]. This displacement angle will significantly degrade the IPF of the power source, especially at low VTRs, which may lead to severe power-factor penalties [19]. Therefore, it is important to consider the IPF compensation problem along with CMV reduction.

Fortunately, a previous study [19] briefly presented a method to compensate IPF for MCs in the zero CMV-SVM method. However, it did not fully investigate all the duty-cycle cases. In addition, the method has not been experimentally verified. To address these issues, this article analyzes all duty cycles under IPF compensation. In the case of negative duty cycles, they will be adjusted to be zero duty cycles so that all duty cycles are positive. This article also determines the maximum IPF that the main power source can achieve according to the VTR. Finally, experiments are carried out to validate the proposed strategy.

NOMENCLATURE

$\mathbf{v_s}$	Three-phase source voltage vector, $[v_{sa}\ v_{sb}\ v_{sc}]^{\mathrm{T}}$
v_{sj}	Instantaneous source phase voltages, $j \in \{a, b, c\}$
V_s	Source voltage amplitude
ω_s	Angular frequency of source voltage
ϕ	Initial phase angle of source voltage
$\vec{v}_s$	Space vector of three-phase source voltage
v_{ij}	Instantaneous input phase voltages of MC, $j \in \{a, b, c\}$
v_K	Instantaneous output phase voltages of MC, $K \in \{A, B, C\}$
V_i, V_o	Amplitudes of MC input and output voltages
α_i, α_o	Phase angles of MC input and output voltages
$\vec{v}_i$, $\vec{v}_o$	Space vectors of MC input and output voltages
i_{ij}	Instantaneous input line currents of MC, $j \in \{a, b, c\}$
i_K	Instantaneous output line currents of MC, $K \in \{A, B, C\}$
I_i, I_o	Amplitudes of MC input and output currents
β_i, β_o	Phase angles of MC input and output currents
$\vec{i}_i$, $\vec{i}_o$	Space vectors of MC input and output currents
d_n	Duty cycles of zero and active vectors, $n \in \{0, 1, 2, 3, 4\}$
q	Voltage transfer ratio of MC, $q = V_o/V_i$
δ_i	Compensated angle, $\delta_i = \angle\vec{v}_i - \angle\vec{i}_i$
$\tilde{\alpha}_o$	Output voltage phase angle referred to the bisecting line of the corresponding sector
$\tilde{\beta}_i$	Input current phase angle referred to the bisecting line of the corresponding sector
$d_{m(0)}$	Duty cycle of rotating vector $\vec{r}_m$ as the zero vector, $m \in \{1, 2, 3, 4, 5, 6\}$
d_M	Total duty cycle of rotating vector $\vec{r}_M$, $M \in \{I, II, III, IV, V, VI\}$ without compensation
$d_M^{'}$	Total duty cycle of rotating vector $\vec{r}_M$, $M \in \{I, II, III, IV, V, VI\}$ under compensation case.
L_f, C_f	Inductance and capacitance of input filter
R_d	Damping resistance of input filter
δ_f	Displacement angle caused by input filter, $\delta_f = \angle\vec{i}_s - \angle\vec{i}_i$
δ_s	Displacement angle at main power supply, $\delta_s = \left\lvert\angle\vec{v}_s - \angle\vec{i}_s\right\rvert$
δ_o	Load displacement angle at output frequency, $\delta_o = \left\lvert\angle\vec{v}_o - \angle\vec{i}_o\right\rvert$
R, L, Z	Load resistance, inductance and impedance
f_o	Output frequency
ω_o	Output angular frequency

II. CONVENTIONAL ZERO CMV-SVM METHOD

Using the symbols defined in Figure 1, let the three-phase source voltage be

$$\mathbf{v_s} = \begin{bmatrix} v_{sa} \\ v_{sb} \\ v_{sc} \end{bmatrix} = V_s \begin{bmatrix} \cos(\omega_s t + \phi) \\ \cos(\omega_s t + \phi - 2\pi/3) \\ \cos(\omega_s t + \phi + 2\pi/3) \end{bmatrix}. \quad (1)$$

According to the space vector theory, three instantaneous source voltages can be represented by one vector $\vec{v}_s$, defined as follows:

$$\vec{v}_s = 2(v_{sa} + v_{sb}e^{j2\pi/3} + v_{sc}e^{j4\pi/3})/3 = V_s e^{j(\omega_s t+\phi)} \quad (2)$$

Similarly, space vectors—representing input voltages, output voltages, input currents, and output currents—are respectively defined as follows:

$$\vec{v}_i = 2(v_{ia} + v_{ib}e^{j2\pi/3} + v_{ic}e^{j4\pi/3})/3 = V_i e^{j\alpha_i} \quad (3)$$
$$\vec{v}_o = 2(v_A + v_B e^{j2\pi/3} + v_C e^{j4\pi/3})/3 = V_o e^{j\alpha_o} \quad (4)$$
$$\vec{i}_i = 2(i_{ia} + i_{ib}e^{j2\pi/3} + i_{ic}e^{j4\pi/3})/3 = I_i e^{j\beta_i} \quad (5)$$
$$\vec{i}_o = 2(i_A + i_B e^{j2\pi/3} + i_C e^{j4\pi/3})/3 = I_o e^{j\beta_o}. \quad (6)$$

Because the MC is supplied by a source voltage and the output load is inductive, the input phases should not be

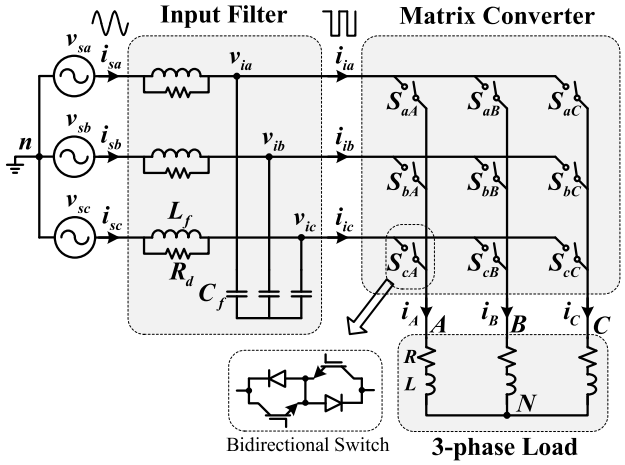

FIGURE 1. A common matrix converter configuration.

TABLE 1. Valid switching states in an MC.

	Switching States				Output Voltage		Input Current	
	No	A	B	C	V_o	α_o	I_i	β_i
Group I	+1	a	b	b	$2v_{ab}/3$	0	$2i_A/\sqrt{3}$	$-\pi/6$
	-1	b	a	a	$-2v_{ab}/3$	0	$-2i_A/\sqrt{3}$	$-\pi/6$
	+2	b	c	c	$2v_{bc}/3$	0	$2i_A/\sqrt{3}$	$\pi/2$
	-2	c	b	b	$-2v_{bc}/3$	0	$-2i_A/\sqrt{3}$	$\pi/2$
	+3	c	a	a	$2v_{ca}/3$	0	$2i_A/\sqrt{3}$	$7\pi/6$
	-3	a	c	c	$-2v_{ca}/3$	0	$-2i_A/\sqrt{3}$	$7\pi/6$
	+4	b	a	b	$2v_{ab}/3$	$2\pi/3$	$2i_B/\sqrt{3}$	$-\pi/6$
	-4	a	b	a	$-2v_{ab}/3$	$2\pi/3$	$-2i_B/\sqrt{3}$	$-\pi/6$
	+5	c	b	c	$2v_{bc}/3$	$2\pi/3$	$2i_B/\sqrt{3}$	$\pi/2$
	-5	b	c	b	$-2v_{bc}/3$	$2\pi/3$	$-2i_B/\sqrt{3}$	$\pi/2$
	+6	a	c	a	$2v_{ca}/3$	$2\pi/3$	$2i_B/\sqrt{3}$	$7\pi/6$
	-6	c	a	c	$-2v_{ca}/3$	$2\pi/3$	$-2i_B/\sqrt{3}$	$7\pi/6$
	+7	b	b	a	$2v_{ab}/3$	$4\pi/3$	$2i_C/\sqrt{3}$	$-\pi/6$
	-7	a	a	b	$-2v_{ab}/3$	$4\pi/3$	$-2i_C/\sqrt{3}$	$-\pi/6$
	+8	c	c	b	$2v_{bc}/3$	$4\pi/3$	$2i_C/\sqrt{3}$	$\pi/2$
	-8	b	b	c	$-2v_{bc}/3$	$4\pi/3$	$-2i_C/\sqrt{3}$	$\pi/2$
	+9	a	a	c	$2v_{ca}/3$	$4\pi/3$	$2i_C/\sqrt{3}$	$7\pi/6$
	-9	c	c	a	$-2v_{ca}/3$	$4\pi/3$	$-2i_C/\sqrt{3}$	$7\pi/6$
Group II	0_a	a	a	a	0	x	0	x
	0_b	b	b	b	0	x	0	x
	0_c	c	c	c	0	x	0	x
Group III	r_1	a	b	c	V_i	α_i	I_o	β_o
	r_2	a	c	b	V_i	$-\alpha_i$	I_o	$-\beta_o$
	r_3	c	a	b	V_i	$2\pi/3+\alpha_i$	I_o	$-2\pi/3+\beta_o$
	r_4	b	a	c	V_i	$2\pi/3-\alpha_i$	I_o	$2\pi/3-\beta_o$
	r_5	b	c	a	V_i	$-2\pi/3+\alpha_i$	I_o	$2\pi/3+\beta_o$
	r_6	c	b	a	V_i	$-2\pi/3-\alpha_i$	I_o	$-2\pi/3-\beta_o$

short-circuited, and the output phases should not be open-circuited [10]. To satisfy these two constraints, there are only 27 valid switching states, corresponding to 27 space vectors, which are listed in Table 1. These switching states are classified into three groups, as follows:

a) Eighteen switching states in Group I produce active vectors, with fixed directions and time-varying amplitudes of the output-voltage and input-current vectors.

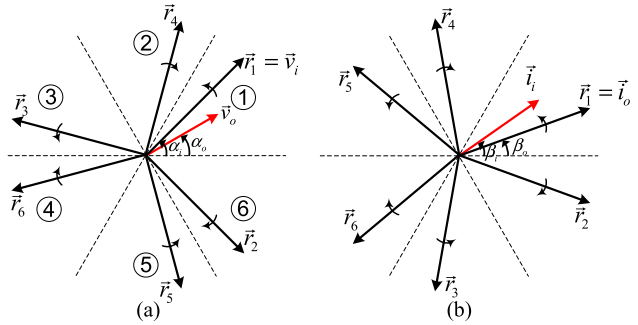

FIGURE 2. (a) Rotating voltage vectors. (b) Rotating current vectors in an MC.

b) Three switching states in Group II produce zero vectors, including zero output-voltage and input-current vectors.

c) Six switching states in Group III produce rotating vectors, with fixed amplitudes and time-varying directions of the output-voltage and input-current vectors.

Among them, the six rotating vectors in group III produce zero CMV [14]–[16]. However, their angular positions always change along with the input voltage, so using these vectors is not simple. Nguyen and Lee, in [1] and [15], proposed a switching pattern using five rotating vectors within a sampling period to control MCs to have zero CMV. Among these five rotating vectors, four vectors act as active vectors to generate the desired output-voltage and input-current vectors, and one rotating vector acts as a zero vector to complete the sampling period. The four selected rotating vectors, which acts as active vectors, and their duty cycles are shown in Table 2 and equations (7)–(10):

$$d_1 = \frac{q}{\sqrt{3}} \times \frac{\sin(2\pi/3 - \tilde{\alpha}_o + \tilde{\beta}_i)}{\cos\delta_i} \tag{7}$$

$$d_2 = \frac{q}{\sqrt{3}} \times \frac{\sin(2\pi/3 - \tilde{\alpha}_o - \tilde{\beta}_i)}{\cos\delta_i} \tag{8}$$

$$d_3 = \frac{q}{\sqrt{3}} \times \frac{\sin(\tilde{\alpha}_o - \tilde{\beta}_i)}{\cos\delta_i} \tag{9}$$

$$d_4 = \frac{q}{\sqrt{3}} \times \frac{\sin(\tilde{\alpha}_o + \tilde{\beta}_i)}{\cos\delta_i} \tag{10}$$

where α_o and β_i are determined from the complex plane, as shown in Figures 2(a) and (b), respectively. The patterns of $\tilde{\alpha}_o$ and $\tilde{\beta}_i$ in the conventional zero CMV-SVM method are shown in Figures 3(a) and (/b), respectively. From Figure 3, the limit of $\tilde{\alpha}_o$ and $\tilde{\beta}_i$ in the conventional zero CMV-SVM method can be obtained as follows:

$$0 \le \tilde{\alpha}_o < \pi/3 \tag{11}$$

$$0 \le \tilde{\beta}_i < \pi/3. \tag{12}$$

The duty cycle of the zero vector can be calculated as follows:

$$\begin{aligned} d_o &= 1 - (d_1 + d_2 + d_3 + d_4) \\ &= 1 - 2q\frac{\cos(\pi/3 - \alpha_o)\cos\beta_i}{\cos\delta_i}. \end{aligned} \tag{13}$$

TABLE 2. Four main rotating vectors selected for the zero CMV-SVM method.

Output-Voltage Vector Sector	Input-Voltage Vector Sector 1				2				3				4				5				6			
1	r_1	r_2	r_3	r_4	r_4	r_5	r_6	r_1	r_5	r_4	r_1	r_6	r_6	r_3	r_2	r_5	r_3	r_6	r_5	r_2	r_2	r_1	r_4	r_3
2	r_4	r_3	r_2	r_1	r_1	r_6	r_5	r_4	r_6	r_1	r_4	r_5	r_5	r_2	r_3	r_6	r_2	r_5	r_6	r_3	r_3	r_4	r_1	r_2
3	r_3	r_4	r_5	r_6	r_6	r_1	r_2	r_3	r_1	r_6	r_3	r_2	r_2	r_5	r_4	r_1	r_5	r_2	r_1	r_4	r_4	r_3	r_6	r_5
4	r_6	r_5	r_4	r_3	r_3	r_2	r_1	r_6	r_2	r_3	r_6	r_1	r_1	r_4	r_5	r_2	r_4	r_1	r_2	r_5	r_5	r_6	r_3	r_4
5	r_5	r_6	r_1	r_2	r_2	r_3	r_4	r_5	r_3	r_2	r_5	r_4	r_4	r_1	r_6	r_3	r_1	r_4	r_3	r_6	r_6	r_5	r_2	r_1
6	r_2	r_1	r_6	r_5	r_5	r_4	r_3	r_2	r_4	r_5	r_2	r_3	r_3	r_6	r_1	r_4	r_6	r_3	r_4	r_1	r_1	r_2	r_5	r_6
Duty cycles	d_I	d_{II}	d_{III}	d_{IV}	d_I	d_{II}	d_{III}	d_{IV}	d_I	d_{II}	d_{III}	d_{IV}	d_I	d_{II}	d_{III}	d_{IV}	d_I	d_{II}	d_{III}	d_{IV}	d_I	d_{II}	d_{III}	d_{IV}

TABLE 3. Rotating vectors selected for the conventional zero CMV-SVM method.

Output Voltage Vector Sector	Input Voltage Vector Sector 1					2					3					4					5					6				
1	r_1	r_2	r_3	r_4	r_5	r_4	r_5	r_6	r_1	r_2	r_5	r_4	r_1	r_6	r_3	r_6	r_3	r_2	r_5	r_4	r_3	r_6	r_5	r_2	r_1	r_2	r_1	r_4	r_3	r_6
2	r_4	r_3	r_2	r_1	r_6	r_1	r_6	r_5	r_4	r_3	r_6	r_1	r_4	r_5	r_2	r_5	r_2	r_3	r_6	r_1	r_2	r_5	r_6	r_3	r_4	r_3	r_4	r_1	r_2	r_5
3	r_3	r_4	r_5	r_6	r_1	r_6	r_1	r_2	r_3	r_4	r_1	r_6	r_3	r_2	r_5	r_2	r_5	r_4	r_1	r_6	r_5	r_2	r_1	r_4	r_3	r_4	r_3	r_6	r_5	r_2
4	r_6	r_5	r_4	r_3	r_2	r_3	r_2	r_1	r_6	r_5	r_2	r_3	r_6	r_1	r_4	r_1	r_4	r_5	r_2	r_3	r_4	r_1	r_2	r_5	r_6	r_5	r_6	r_3	r_4	r_1
5	r_5	r_6	r_1	r_2	r_3	r_2	r_3	r_4	r_5	r_6	r_3	r_2	r_5	r_4	r_1	r_4	r_1	r_6	r_3	r_2	r_1	r_4	r_3	r_6	r_5	r_6	r_5	r_2	r_1	r_4
6	r_2	r_1	r_6	r_5	r_4	r_5	r_4	r_3	r_2	r_1	r_4	r_5	r_2	r_3	r_6	r_3	r_6	r_1	r_4	r_5	r_6	r_3	r_4	r_1	r_2	r_1	r_2	r_5	r_6	r_3
Duty cycles	d_I	d_{II}	d_{III}	d_{IV}	d_V	d_I	d_{II}	d_{III}	d_{IV}	d_V	d_I	d_{II}	d_{III}	d_{IV}	d_V	d_I	d_{II}	d_{III}	d_{IV}	d_V	d_I	d_{II}	d_{III}	d_{IV}	d_V	d_I	d_{II}	d_{III}	d_{IV}	d_V

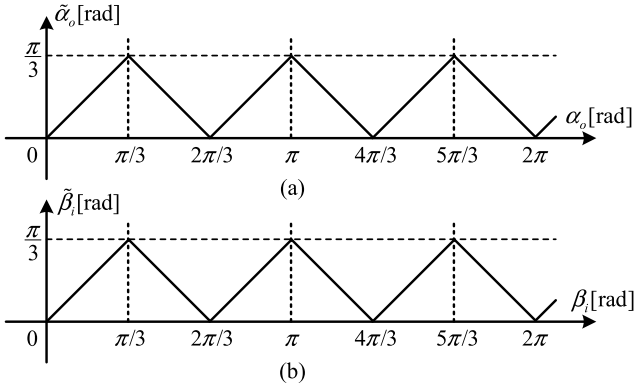

FIGURE 3. (a) Relationship between $\tilde{\alpha}_o$ and α_o. (b) Relationship between $\tilde{\beta}_i$ and β_i in the zero CMV-SVM method.

The zero vector can be executed using a set of three counterclockwise-rotating vectors (i.e., $\vec{r}_1$, $\vec{r}_3$, $\vec{r}_5$) or clockwise-rotating (i.e., $\vec{r}_2$, $\vec{r}_4$, $\vec{r}_6$) vectors with the same duty cycle:

$$\vec{0} = \frac{\vec{r}_1 + \vec{r}_3 + \vec{r}_5}{3} = \frac{\vec{r}_2 + \vec{r}_4 + \vec{r}_6}{3}. \tag{14}$$

In the case of no compensation ($\delta_i = 0$), with the limits of $\tilde{\alpha}_o$ and $\tilde{\beta}_i$ in (11) and (12), respectively, only duty cycle d_3 can be negative. To ensure that the duty cycle d_3 of rotating vector $\vec{r}_3$ is non-negative, the zero vector should be implemented using a set of three counterclockwise-rotating vectors, i.e., $\vec{0} = (\vec{r}_1 + \vec{r}_3 + \vec{r}_5)/3$. This means that, in addition to creating a main active vector as shown in (7)–(10), the rotating vectors $\vec{r}_1$, $\vec{r}_3$, and $\vec{r}_5$ must execute an extra interval to create the zero vector, as follows:

$$d_{1(0)} = \frac{d_0}{3} \tag{15}$$

$$d_{3(0)} = \frac{d_0}{3} \tag{16}$$

$$d_{5(0)} = \frac{d_0}{3}. \tag{17}$$

Therefore, in the conventional method, rotating vectors are finally selected as shown in Table 3, and their duty cycles are determined as follows:

$$d_I = d_1 + d_{1(0)} \tag{18}$$

$$d_{II} = d_2 \tag{19}$$

$$d_{III} = d_3 + d_{3(0)} \tag{20}$$

$$d_{IV} = d_4 \tag{21}$$

$$d_V = d_{5(0)}. \tag{22}$$

Substituting (7)–(10), (13), and (15)–(17) into (18)–(22), we obtain (23)–(27):

$$d_I = \frac{1}{3}\left[1 - 2q\cos(2\pi/3 - \tilde{\alpha}_o)\cos(\pi/3 + \tilde{\beta}_i)\right] \tag{23}$$

$$d_{II} = \frac{q}{\sqrt{3}}\sin(2\pi/3 - \tilde{\alpha}_o - \tilde{\beta}_i) \tag{24}$$

$$d_{III} = \frac{1}{3}\left[1 - 2q\cos\tilde{\alpha}_o\cos(\pi/3 - \tilde{\beta}_i)\right] \tag{25}$$

$$d_{IV} = \frac{q}{\sqrt{3}}\sin(\tilde{\alpha}_o + \tilde{\beta}_i) \tag{26}$$

$$d_V = \frac{1}{3}\left[1 - 2q\cos(\pi/3 - \tilde{\alpha}_o)\cos\tilde{\beta}_i\right]. \tag{27}$$

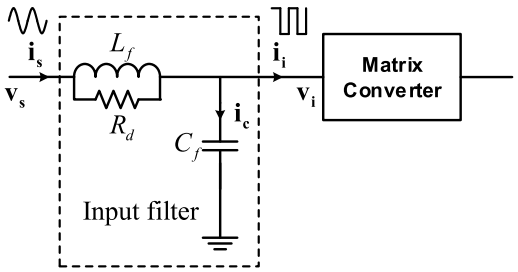

FIGURE 4. Equivalent circuit of input filter.

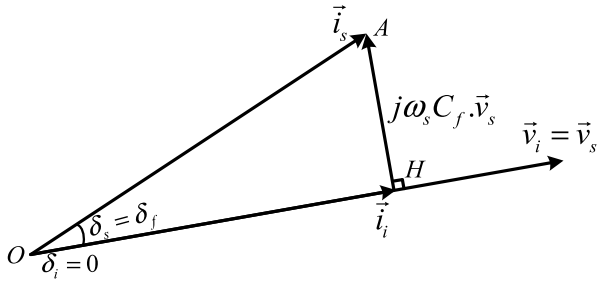

FIGURE 5. Vector diagram of input voltages and currents at the input filter with no compensation.

With the limits of $\tilde{\alpha}_o$ and $\tilde{\beta}_i$ in (11) and (12), it is possible to prove that all duty cycles—d_I, d_{II}, d_{III}, d_{IV}, and d_V—in (23)–(27) are non-negative.

All of these duty cycles must be less than 1, so the VTR in the conventional zero CMV-SVM method is limited as follows:

$$q \leq \frac{1}{2} \tag{28}$$

III. PROPOSED IPF STRATEGY FOR ZERO CMV-SVM METHOD

A. INPUT FILTER ANALYSIS

The input filter is a crucial component in a practical MC system, which is used to smooth the source current. However, it creates a displacement angle between current and voltage, leading to a low IPF. Therefore, it is important to study this displacement angle to improve the IPF. In MC systems, a second-order *LC* filter with a damping resistor is commonly used, as shown in Figure 4. From Figure 4, in the condition of $R_d \gg \omega_s L_f$, the relationship between ($\vec{v}_i$, $\vec{i}_i$) and ($\vec{v}_s$, $\vec{i}_s$)can be written as follows:

$$\vec{i}_i = \vec{i}_s - j\omega_s C_f \vec{v}_s \tag{29}$$

$$\vec{v}_i = \vec{v}_s - j\omega_s L_f \vec{i}_s. \tag{30}$$

Because the voltage drop at the input filter is very small in comparison to the source voltage, the input voltage of the MC and the source voltage are considered to be equal [19]:

$$\vec{v}_i = \vec{v}_s. \tag{31}$$

From (29) and (31), we can draw the vector diagram of input voltages and currents at the input filter, as shown in Figure 5. From Figure 5, it is possible to determine the displacement angle caused by the input filter as follows:

$$\sin \delta_f = \frac{\omega_s C_f V_s}{I_s}. \tag{32}$$

In addition, based on the law of conservation of energy, we have the following:

$$V_s I_s \cos \delta_s = V_o I_o \cos \delta_o \tag{33}$$

where $V_o = qV_i = qV_s$; $I_o = \frac{V_o}{Z} = \frac{qV_s}{Z}$; $\cos \delta_o = \frac{R}{Z}$.

Therefore, equation (33) is rewritten as follows:

$$I_s = \frac{q^2 V_s R}{Z^2 \cos \delta_s} \tag{34}$$

Combining (32) and (34), the displacement angle caused by the input filter can be determined by the MC parameters as follows:

$$\tan \delta_f = \frac{\omega_s C_f Z^2}{q^2 R} \tag{35}$$

The following strategy will attempt to compensate the angle δ_f in (35) as much as possible to achieve the maximum IPF of the power source.

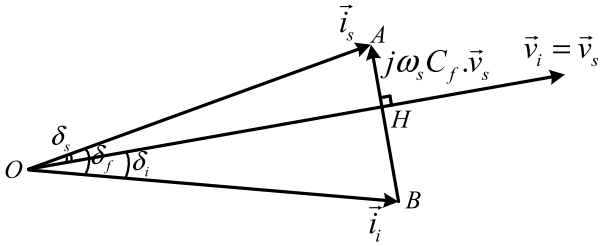

FIGURE 6. Vector diagram of input voltages and currents at the input filter with compensated angle δ_i.

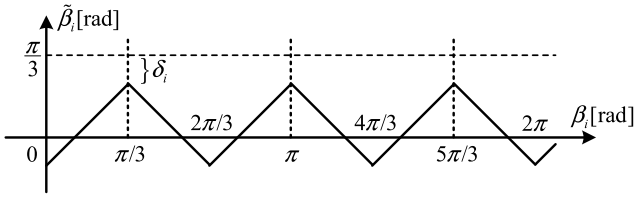

FIGURE 7. Relationship between $\tilde{\beta}_i$ and β_i in the zero CMV-SVM method with the proposed IPF strategy.

B. PROPOSED IPF COMPENSATION STRATEGY

Since the vector $\vec{v}_i$ is definite ($\vec{v}_i = \vec{v}_s$) and uncontrollable, the angle δ_f in (35) can only be compensated by controlling the vector $\vec{i}_i$. Based on Figure 5, to compensate the angle δ_f, the vector $\vec{i}_i$ must be delayed by an angle δ_i in comparison to $\vec{v}_i$, as shown in Figure 6. Therefore, the phase angle of the input current vector is determined as $\beta_i = \alpha_i - \delta_i$. The patterns of $\tilde{\beta}_i$ are depicted in Figure 7 using the following limit:

$$-\pi/3 \leq \tilde{\beta}_i < \pi/3 \tag{36}$$

TABLE 4. Rotating vectors selected for the zero CMV-SVM method with the proposed IPF strategy.

Output Voltage Vector Sector	Input Voltage Vector Sector 1					2					3					4					5					6				
1	r_1	r_2	r_3	r_4	r_6	r_4	r_5	r_6	r_1	r_3	r_5	r_4	r_1	r_6	r_2	r_6	r_3	r_2	r_5	r_1	r_3	r_6	r_5	r_2	r_4	r_2	r_1	r_4	r_3	r_5
2	r_4	r_3	r_2	r_1	r_5	r_1	r_6	r_5	r_4	r_2	r_6	r_1	r_4	r_5	r_3	r_5	r_2	r_3	r_6	r_4	r_2	r_5	r_6	r_3	r_1	r_3	r_4	r_1	r_2	r_6
3	r_3	r_4	r_5	r_6	r_2	r_6	r_1	r_2	r_3	r_5	r_1	r_6	r_3	r_2	r_4	r_2	r_5	r_4	r_1	r_3	r_5	r_2	r_1	r_4	r_6	r_4	r_3	r_6	r_5	r_1
4	r_6	r_5	r_4	r_3	r_1	r_3	r_2	r_1	r_6	r_4	r_2	r_3	r_6	r_1	r_5	r_1	r_4	r_5	r_2	r_6	r_4	r_1	r_2	r_5	r_3	r_5	r_6	r_3	r_4	r_2
5	r_5	r_6	r_1	r_2	r_4	r_2	r_3	r_4	r_5	r_1	r_3	r_2	r_5	r_4	r_6	r_4	r_1	r_6	r_3	r_5	r_1	r_4	r_3	r_6	r_2	r_6	r_5	r_2	r_1	r_3
6	r_2	r_1	r_6	r_5	r_3	r_5	r_4	r_3	r_2	r_6	r_4	r_5	r_2	r_3	r_1	r_3	r_6	r_1	r_4	r_2	r_6	r_3	r_4	r_1	r_5	r_1	r_2	r_5	r_6	r_4
Duty cycles	d_I'	d_{II}'	d_{III}'	d_{IV}'	d_V'	d_I'	d_{II}'	d_{III}'	d_{IV}'	d_V'	d_I'	d_{II}'	d_{III}'	d_{IV}'	d_V'	d_I'	d_{II}'	d_{III}'	d_{IV}'	d_V'	d_I'	d_{II}'	d_{III}'	d_{IV}'	d_V'	d_I'	d_{II}'	d_{III}'	d_{IV}'	d_V'

Under this condition, from (7) to (10), duty cycles d_3 and d_4 may be negative:

i) d_3 is negative when $\tilde{\beta}_i > \tilde{\alpha}_o \geq 0$

ii) d_4 is negative when $\tilde{\beta}_i < -\tilde{\alpha}_o \leq 0$

Therefore, it is clear that d_3 and d_4 cannot be negative at the same time. In light of this, the present paper proposes a strategy as follows:

i) When $d_4 > 0$, the selected vectors and their duty cycles are the same as those in the conventional case.

ii) When $d_4 < 0$, to ensure that the duty cycle d_4 of the rotating vector $\vec{r}_4$ is non-negative, the zero vector should be implemented by a set of three clockwise-rotating vectors, i.e., $\vec{0} = (\vec{r}_2+\vec{r}_4+\vec{r}_6)/3$. Therefore, in addition to creating the main active vector as shown in (7)–(10), the rotating vectors $\vec{r}_2$, $\vec{r}_4$, and $\vec{r}_6$ must execute an extra interval to create the zero vector, as follows:

$$d_{2(0)} = \frac{d_0}{3} \tag{37}$$

$$d_{4(0)} = \frac{d_0}{3} \tag{38}$$

$$d_{6(0)} = \frac{d_0}{3}. \tag{39}$$

The selected rotating vectors are shown in Table 4 and their duty cycles are calculated as follows:

$$d_I' = d_1 \tag{40}$$

$$d_{II}' = d_2 + d_{2(0)} \tag{41}$$

$$d_{III}' = d_3 \tag{42}$$

$$d_{IV}' = d_4 + d_{4(0)} \tag{43}$$

$$d_V' = d_{6(0)}. \tag{44}$$

Substituting (7)–(10), (13), and (37)–(39) into (40)–(44), it is possible to obtain the following results:

$$d_I' = \frac{q}{\sqrt{3}} \times \frac{\sin(2\pi/3 - \tilde{\alpha}_o + \tilde{\beta}_i)}{\cos\delta_i} \tag{45}$$

$$d_{II}' = \frac{1}{3}\left[1 - 2q\frac{\cos(2\pi/3 - \tilde{\alpha}_o)\cos(\pi/3 - \tilde{\beta}_i)}{\cos\delta_i}\right] \tag{46}$$

$$d_{III}' = \frac{q}{\sqrt{3}} \times \frac{\sin(\tilde{\alpha}_o - \tilde{\beta}_i)}{\cos\delta_i} \tag{47}$$

$$d_{IV}' = \frac{1}{3}\left[1 - 2q\frac{\cos\tilde{\alpha}_o\cos(\pi/3 + \tilde{\beta}_i)}{\cos\delta_i}\right] \tag{48}$$

$$d_V' = \frac{1}{3}\left[1 - 2q\frac{\cos(\pi/3 - \tilde{\alpha}_o)\cos\tilde{\beta}_i}{\cos\delta_i}\right] \tag{49}$$

In the case of $d_4 < 0$, which implies that $\tilde{\beta}_i < 0$, it is possible to prove that all duty cycles in (45)–(49) are positive, so the zero CMV-SVM method can be implemented in this case.

The limit of VTR in the zero CMV-SVM method with the compensated angle δ_i is:

$$q \leq \frac{1}{2}\cos\delta_i \tag{50}$$

C. MAXIMUM COMPENSABLE ANGLE AND MAXIMUM IPF

Even though the proposed IPF compensation strategy attempts to compensate the angle δ_f in (35) as much as possible to achieve the maximum IPF of the power source, it is not always possible to compensate all values of δ_f to achieve unity IPF. This section covers the conditions for the MC to achieve unity IPF, and the maximum allowable IPF value when unity cannot be reached.

1) CONDITION TO ACHIEVE UNITY IPF

According to [20], the relationship between δ_s, δ_i and δ_f is:

$$\tan\delta_s + \tan\delta_i = \tan\delta_f. \tag{51}$$

To obtain the unity IPF ($\delta_s = 0$), from (35) and (51), the compensated angle $\delta_i$must be:

$$\tan\delta_i = \tan\delta_f = \frac{\omega_s C_f Z^2}{q^2 R}. \tag{52}$$

Let the quality factor Q be defined as

$$Q^2 = \frac{\omega_s C_f Z^2}{R}. \tag{53}$$

From (50), (52), and (53), the condition for MC to achieve unity IPF using the zero CM-SVM method is:

$$\begin{cases} \tan\delta_i = \dfrac{Q^2}{q^2} \\ \cos\delta_i \geq 2q \end{cases} \tag{54}$$

where $Q^2 = \frac{\omega_s C_f Z^2}{R}$.

TABLE 5. System parameters.

Power supply	Input filter	Output load
$V_s = 100V$ $f_i = 60$ Hz	$L_f = 1.4$ mH $C_f = 22\ \mu$F $R_d = 20\ \Omega$	$R = 10\ \Omega$ $L = 15$ mH $f_o = 50$ Hz

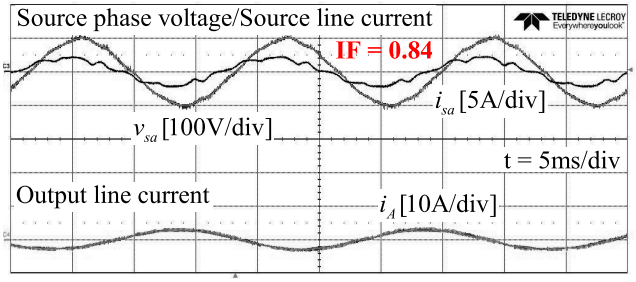

FIGURE 8. Source phase voltage/source line current and output line current at $q = 0.4$ in the zero CMV-SVM method without compensation.

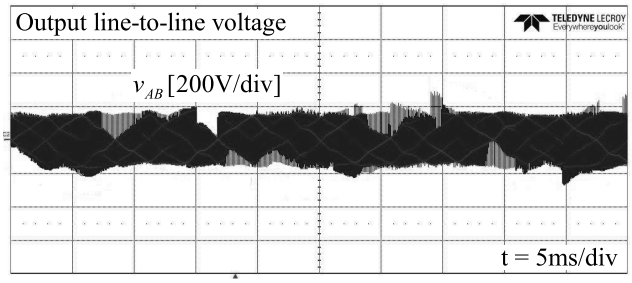

FIGURE 9. Output line-to-line voltage at $q = 0.4$ in the zero CMV-SVM method without compensation.

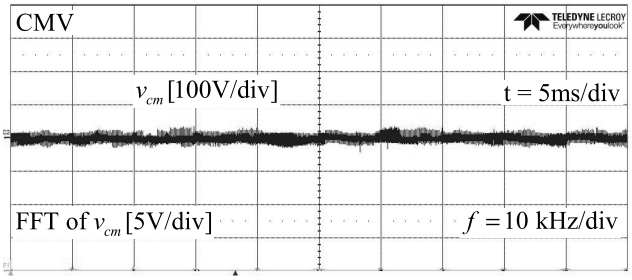

FIGURE 10. CMV waveform and its FFT at $q = 0.4$ in the zero CMV-SVM method without compensation.

From (54), it is possible to derive the following condition:

$$\begin{aligned} &\tan^2\delta_i + 1 = \frac{1}{\cos^2\delta_i} \\ &\Rightarrow \left(\frac{Q^2}{q^2}\right)^2 + 1 = \frac{1}{\cos^2\delta_i} \le \frac{1}{(2q)^2} \\ &\Rightarrow q^4 - \frac{1}{4}q^2 + Q^4 \le 0. \end{aligned} \tag{55}$$

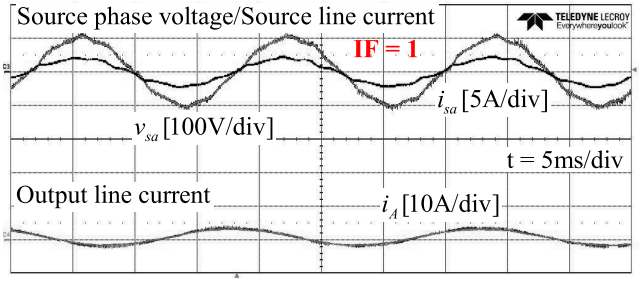

FIGURE 11. Source phase voltage/source line current and output line current at $q = 0.4$ in the zero CMV-SVM method with the proposed IPF compensation strategy.

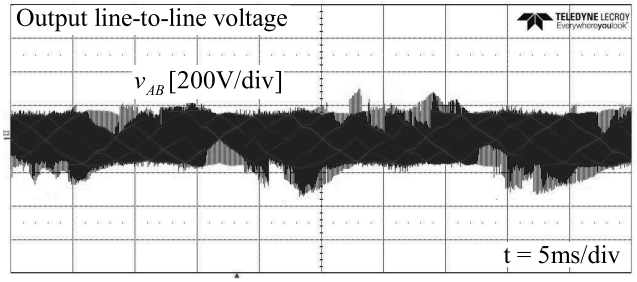

FIGURE 12. Output line-to-line voltage at $q = 0.4$ in the zero CMV-SVM method with the proposed IPF compensation strategy.

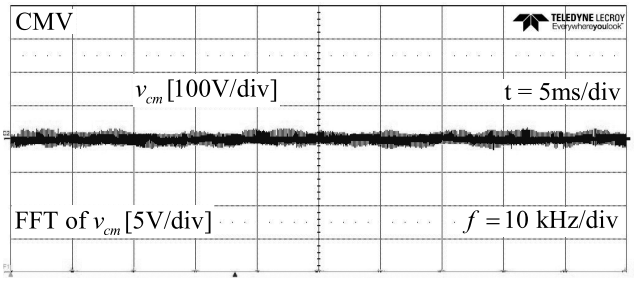

FIGURE 13. CMV waveform and its FFT at $q = 0.4$ in the zero CMV-SVM method with the proposed IPF compensation strategy.

From (55), we can finally determine the condition to achieve unity IPF for MCs as follows:

$$\begin{cases} \sqrt{\frac{1}{8} - \sqrt{\left(\frac{1}{8}\right)^2 - Q^4}} \le q \le \sqrt{\frac{1}{8} + \sqrt{\left(\frac{1}{8}\right)^2 - Q^4}} \\ Q^2 = \dfrac{\omega_s C_f Z^2}{R} \le \dfrac{1}{8} \end{cases} \tag{56}$$

2) MAXIMUM ALLOWABLE IPF

When the condition in (56) is not satisfied, the MC cannot achieve unity IPF, and it is necessary to determine the maximum allowable IPF. In this case, from (50) and (51), we have the following relationship:

$$\begin{cases} \tan\delta_s + \tan\delta_i = \tan\delta_f = \dfrac{Q^2}{q^2} \\ \cos\delta_i \ge 2q \end{cases} \tag{57}$$

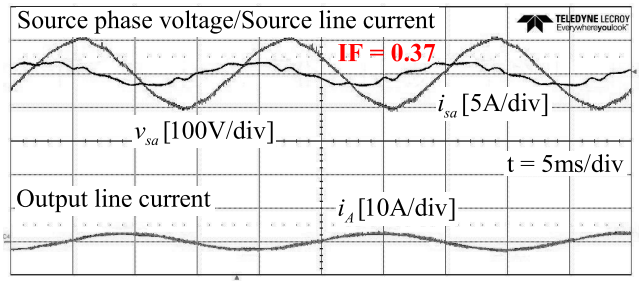

FIGURE 14. Source phase voltage/source line current and output line current at $q = 0.2$ in the zero CMV-SVM method without compensation.

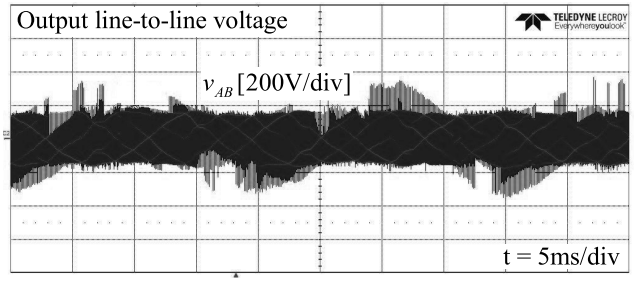

FIGURE 15. Output line-to-line voltage at $q = 0.2$ in the zero CMV-SVM method without compensation.

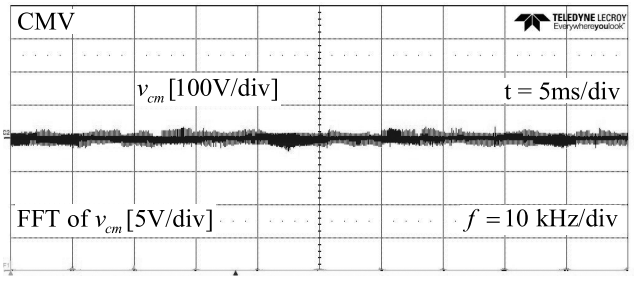

FIGURE 16. CMV waveform and its FFT at $q = 0.2$ in the zero CMV-SVM method without compensation.

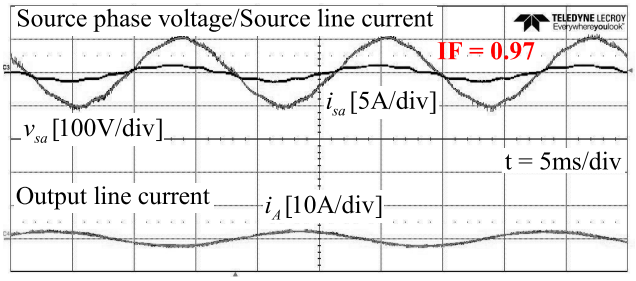

FIGURE 17. Source phase voltage/source line current and output line current at $q = 0.2$ in the zero CMV-SVM method with the proposed IPF compensation strategy.

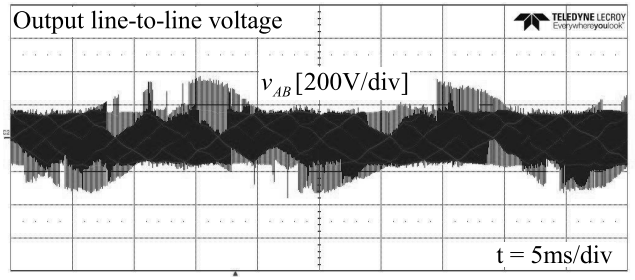

FIGURE 18. Output line-to-line voltage at $q = 0.2$ in the zero CMV-SVM method with the proposed IPF compensation strategy.

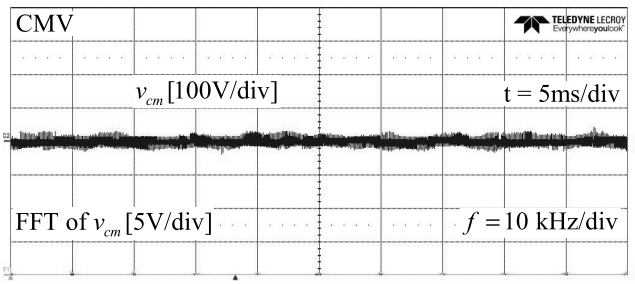

FIGURE 19. CMV waveform and its FFT at $q = 0.2$ in the zero CMV-SVM method with the proposed IPF compensation strategy.

To achieve the maximum allowable IPF, the compensated angle must be maximized, thus: $\cos\delta_i = 2q$. Therefore, it is possible to calculate:

$$\tan\delta_i = \frac{\sqrt{1-4q^2}}{2q} = \sqrt{\frac{1}{4q^2}-1} \tag{58}$$

From (57) and (58), it is possible to calculate:

$$\tan\delta_s = \frac{Q^2}{q^2} - \sqrt{\frac{1}{4q^2}-1} \tag{59}$$

Finally, the maximum allowable IPF can be determined as follows:

$$\mathrm{IPF}^2 = \cos^2\delta_s = \frac{q^4}{Q^4 - 2Q^2q^2\sqrt{\frac{1}{4q^2}-1} + \frac{q^2}{4}} \tag{60}$$

IV. EXPERIMENTAL RESULTS

To verify the proposed theoretical study, experiments for the proposed IPF strategy are carried out using a three-phase power supply, *LC* filter, and a three-phase symmetrical passive *RL* load with the parameters shown in Table 5. The switching frequency is 10 kHz. The MC was built using 18 insulated-gate bipolar transistors (IRG4PF50WD). Main control was implemented using fixed-point digital signal processors (TMS320F2812). A complex programmable logic device (EPM7128SLC84-15) was used for four-step commutation.

With the parameters in Table 5, condition (56) to achieve unity IPF for MCs, in this case, will be:

$$\begin{cases} 0.238 \le q \le 0.445 \\ Q^2 = 0.1 \le \frac{1}{8} = 0.125 \end{cases} \Rightarrow 0.238 \le q \le 0.445 \tag{61}$$

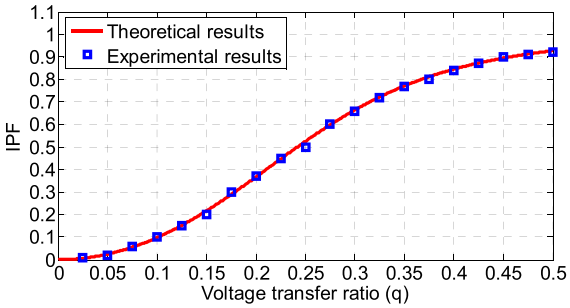

FIGURE 20. Theoretical and experimental results of IPF in the zero CMV-SVM method without compensation.

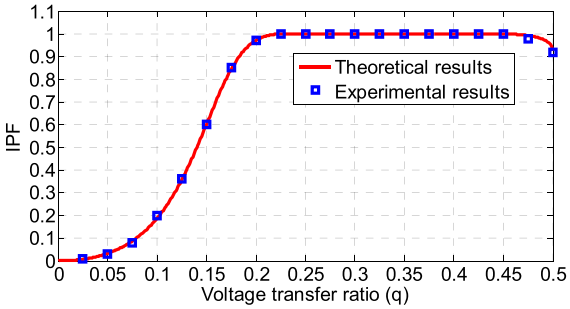

FIGURE 21. Theoretical and experimental results of IPF in the zero CMV-SVM method with the proposed IPF compensation strategy.

Figures 8 and 9 show the MC input and output waveforms when using the zero CMV-SVM method without compensation at $q = 0.4$. In this case, the IPF achieved is 0.84. The CMV is almost zero, other than a small amount of noise owing to the commutation process [1], as shown in Figure 10.

Subsequently, the maximum compensated angle is applied to the zero CMV-SVM method; the MC input and output waveforms are shown in Figures 11 and 12, respectively. As can be seen, $q = 0.4$ meets the condition in (61), so the MC can achieve unity IPF in this case. The proposed IPF compensation strategy does not affect the results of the CMV, and it can be seen that the CMV is nearly zero in Figure 13.

When the MC operates at a low voltage transfer ratio, i.e., $q = 0.2$, the IPF is only 0.37, as shown in Figures 14 and 15. Since $q = 0.2$ does not satisfy the condition in (61), the MC cannot achieve unity IPF. Therefore, after applying the maximum compensated angle, the MC only achieves a maximum IPF of 0.97, as shown in Figures 17 and 18. It is clear that this value is in good agreement with the theoretical predictions in (60). Because the zero CMV modulation method is used, the CMV is always almost zero, as shown in Figures 16 and 19, for both uncompensated and compensated cases.

The IPF results in other cases of VTR, within the range of 0 to 0.5, are shown in Figures 20 and 21 without compensation and the proposed IPF compensation strategy, respectively. It can be seen from Figures 20 and 21 that experimental results are in good agreement with the proposed theoretical results.

V. CONCLUSION

This article has presented an IPF compensation strategy for the zero CMV-SVM method. The proposed strategy investigated the displacement angle caused by the input filter and its effect on the value of duty cycles upon compensation. The proposed strategy decides which rotating vectors are synthesized into zero vectors, thereby making all duty cycles non-negative, allowing the zero CMV-SVM method to be applied. This article also specifies when the main power source can achieve unity IPF and the maximum allowable IPF according to the VTR. Experimental results confirmed that the MC's IPF is in good agreement with the proposed theoretical results.

REFERENCES

[1] H.-N. Nguyen and H.-H. Lee, "An enhanced SVM method to drive matrix converters for zero common-mode voltage," *IEEE Trans. Power Electron.*, vol. 30, no. 4, pp. 1788–1792, Apr. 2015.

[2] A. Tsoupos and V. Khadkikar, "A novel SVM technique with enhanced output voltage quality for indirect matrix converters," *IEEE Trans. Ind. Electron.*, vol. 66, no. 2, pp. 832–841, Feb. 2019.

[3] T. Friedli and J. W. Kolar, "Milestones in matrix converter research," *IEEJ J. Ind. Appl.*, vol. 1, no. 1, pp. 2–14, 2012.

[4] T. F. Podlesak, D. C. Katsis, P. W. Wheeler, J. C. Clare, L. Empringham, and M. Bland, "A 150-kVA vector-controlled matrix converter induction motor drive," *IEEE Trans. Ind. Appl.*, vol. 41, no. 3, pp. 841–847, May 2005.

[5] H.-N. Nguyen and H.-H. Lee, "A DSVM method for matrix converters to suppress common-mode voltage with reduced switching losses," *IEEE Trans. Power Electron.*, vol. 31, no. 6, pp. 4020–4030, Jun. 2016.

[6] V. Padhee, A. K. Sahoo, and N. Mohan, "Modulation techniques for enhanced reduction in common-mode voltage and output voltage distortion in indirect matrix converters," *IEEE Trans. Power Electron.*, vol. 32, no. 11, pp. 8655–8670, Nov. 2017.

[7] M. J. Duran, J. A. Riveros, F. Barrero, H. Guzman, and J. Prieto, "Reduction of common-mode voltage in five-phase induction motor drives using predictive control techniques," *IEEE Trans. Ind. Appl.*, vol. 48, no. 6, pp. 2059–2067, Nov. 2012.

[8] A. Tsoupos and V. Khadkikar, "A novel SVM technique with enhanced output voltage quality for indirect matrix converters," *IEEE Trans. Ind. Electron.*, vol. 66, no. 2, pp. 832–842, Feb. 2019.

[9] T. D. Nguyen and H.-H. Lee, "A new SVM method for an indirect matrix converter with common-mode voltage reduction," *IEEE Trans. Ind. Informat.*, vol. 10, no. 1, pp. 61–72, Feb. 2014.

[10] H.-N. Nguyen and H.-H. Lee, "An effective SVM method for matrix converters with a superior output performance," *IEEE Trans. Ind. Electron.*, vol. 65, no. 9, pp. 6948–6958, Sep. 2018.

[11] H. M. Nguyen, H.-H. Lee, and T.-W. Chun, "A novel method of common-mode voltage reduction in matrix converters," *Int. J. Electron.*, vol. 99, no. 1, pp. 1–14, Jan. 2012.

[12] J. Espina, C. Ortega, L. de Lillo, L. Empringham, J. Balcells, and A. Arias, "Reduction of output common mode voltage using a novel SVM implementation in matrix converters for improved motor lifetime," *IEEE Trans. Ind. Electron.*, vol. 61, no. 11, pp. 5903–5911, Nov. 2014.

[13] H.-H. Lee and H. M. Nguyen, "An effective direct-SVM method for matrix converters operating with low-voltage transfer ratio," *IEEE Trans. Power Electron.*, vol. 28, no. 2, pp. 920–929, Feb. 2013.

[14] Q. Guan, P. W. Wheeler, Q. Guan, and P. Yang, "Common-mode voltage reduction for matrix converters using all valid switch states," *IEEE Trans. Power Electron.*, vol. 31, no. 12, pp. 8247–8259, Dec. 2016.

[15] H.-N. Nguyen and H.-H. Lee, "A modulation scheme for matrix converters with perfect zero common-mode voltage," *IEEE Trans. Power Electron.*, vol. 31, no. 8, pp. 5411–5422, Aug. 2016.

[16] J. Lei, S. Feng, B. Zhou, H.-N. Nguyen, J. Zhao, and W. Chen, "Simple modulation scheme with zero common-mode voltage and improved efficiency for direct matrix converter fed PMSM drives," *IEEE J. Emerg. Sel. Topics Power Electron.*, early access, Aug. 12, 2019, doi: 10.1109/JESTPE.2019.2934730.

[17] H. She, H. Lin, X. Wang, and L. Yue, "Damped input filter design of matrix converter," in *Proc. Int. Conf. Power Electron. Drive Syst.*, Nov. 2009, pp. 672–677.
[18] H. M. Nguyen, H.-H. Lee, and T.-W. Chun, "Input power factor compensation algorithms using a new direct-SVM method for matrix converter," *IEEE Trans. Ind. Electron.*, vol. 58, no. 1, pp. 232–243, Jan. 2011.
[19] H.-N. Nguyen, T. D. Nguyen, and H.-H. Lee, "A modulation strategy to eliminate CMV for matrix converters with input power factor compensation," in *Proc. 42nd Annu. Conf. IEEE Ind. Electron. Soc. (IECON)*, Oct. 2016, pp. 6237–6242.
[20] H.-N. Nguyen, M.-K. Nguyen, T.-D. Duong, T.-T. Tran, Y.-C. Lim, and J.-H. Choi, "A study on input power factor compensation capability of matrix converters," *Electronics*, vol. 9, pp. 82–99, Jan. 2020.

HUU-NHAN NGUYEN (Member, IEEE) received the B.S. degree in electrical engineering from the Ho Chi Minh City University of Technology, Vietnam, in 2010, and the Ph.D. degree in electrical engineering from the University of Ulsan, South Korea, in 2017.

He currently works with the Institute of Research and Development (IRD), Duy Tan University, Da Nang, Vietnam, where he is also engaged in teaching and research in the areas of automatic control and power electronics. His research interests include power conversion, advanced controls, and electrical machine drives.

MINH-KHAI NGUYEN (Senior Member, IEEE) received the B.S. degree in electrical engineering from the Ho Chi Minh City University of Technology, Ho Chi Minh City, Vietnam, in 2005, and the M.S. and Ph.D. degrees in electrical engineering from Chonnam National University, Gwangju, South Korea, in 2007 and 2010, respectively. He was a Lecturer with the Ho Chi Minh City University of Technology and Education, Ho Chi Minh City, and an Assistant Professor with Chosun University, Gwangju, and the Queensland University of Technology, Australia. He is currently with the Department of Electrical and Computer Engineering, Wayne State University, Detroit, MI, USA. His current research interests include power electronics converters for renewable energy systems and electric vehicles. He has served as a Guest Associate Editor for the IEEE TRANSACTIONS ON POWER ELECTRONICS Special Issue on the Impedance Source Converter Topologies and Applications. He is also an Associate Editor of the *Journal of Power Electronics* and the *International Journal of Power Electronics*.

VAN-QUANG-BINH NGO received the M.Sc. degree from the Da Nang University of Technology, Vietnam, in 2009, and the Ph.D. degree from the CentraleSupélec, University of Paris-Saclay, France, in 2017, all in automation. He was appointed as a Lecturer with the Hue University of Education, Vietnam, in 2004, where he was promoted to an Assistant Professor, in 2017. He was a Postdoctoral Researcher with the Department of Electrical Engineering, Chonnam National University, South Korea, in 2018. His research interests include multilevel converters topology and predictive control for power converters and electrical drives and their applications in renewable energy systems.

TAN-TAI TRAN received the B.S. degree in electrical and electronic engineering technology and the M.S. degree in electronic engineering from the Ho Chi Minh City University of Technology and Education, Ho Chi Minh City, Vietnam, in 2012 and 2016, respectively, and the Ph.D. degree in electrical engineering from Chonnam National University, Gwangju, South Korea, in 2020. He is currently with the Department of Electrical Engineering, Chonnam National University. His current research interests include renewable energy systems, automation systems, dc–dc converters, and dc–ac inverters.

JOON-HO CHOI (Member, IEEE) received the B.S., M.S., and Ph.D. degrees in electrical engineering from Soongsil University, Seoul, South Korea, in 1996, 1998, and 2002, respectively. Since 2003, he has been a Professor with Chonnam National University, Gwangju, South Korea. His research interests include operation and integration and control strategies of distributed generation, distribution automation, and modeling and operation algorithms of the smart grid. He is a Life Member of KIEE and the Korean Institute of Illuminating and Electrical Installation Engineers and a Committee Member of IBS, South Korea. Since 2004, he has been an Associate Editor of the *Transactions of the KIEE*.

YOUNG-CHEOL LIM (Member, IEEE) was born in Chonnam, South Korea, in 1953. He received the B.S. degree in electrical engineering from Chonnam National University, Gwangju, South Korea, in 1975, and the M.S. and Ph.D. degrees from Korea University, Seoul, South Korea, in 1977 and 1990, respectively.

In 1981, he became a Professor with Chonnam National University, where he was the Director of the Research Center for High-Quality Electric Components and Systems, from 1998 to 2007. He is currently a Distinguished Research Emeritus Professor with Chonnam National University. He is a coauthor of three books. He has authored or coauthored more than 200 published technical articles. His current research interests include power electronics, control instruments, and neurofuzzy control. He received a number of awards, including the 2000 Korean Institute of Power Electronics (KIPE) Best Paper Award and the 2001 KIPE Academic Award. He was the President of KIPE, in 2009. He has been involved in various academic societies, such as KIPE, the Korean Institute of Electrical Engineers, and the Institute of Control, Automation, and Systems Engineers, South Korea.